ZOOLOGICAL SCIENCE 2: 641–651 (1985)

Crayfish Local Bilateral Spiking Interneurons: Role in Contralateral Uropod Motor Pattern Formation

TOSHIKI NAGAYAMA and MITUHIKO HISADA

Zoological Institute, Faculty of Science, Hokkaido University, Sapporo 060, Japan

ABSTRACT—Both touching the exopodite and stimulating electrically the second root afferents of the terminal abdominal ganglion of the crayfish *Procambarus clarkii* Girard caused the reciprocal activation of the contralateral uropod motoneurons: spontaneous discharge rate of the closer Red MN No. 1 increased and that of opener motoneurons decreased. This reciprocal motor pattern was formed by the local circuitry within the terminal abdominal ganglion. Since neither the second root afferents nor the motoneuron dendrites did cross the midline of the ganglion, transmission of sensory inputs across the midline was investigated by intracellular current injection and staining of related neurons. We found local bilateral spiking interneurons (LBSNs) which extended their branches bilaterally in the ganglion. They received excitatory inputs, presumably monosynaptically, from the second root afferents on their somata side. They could form the reciprocal activity of the antagonistic uropod motoneurons on the contralateral side to their somata when current was injected intracellularly. Artificial depolarization of the LBSNs increased spike activity of the Red MN No. 1 and decreased that of opener motoneurons. We hence concluded that the LBSNs transmit the sensory inputs to the contralateral uropod motoneurons. Four types of structurally and physiologically distinct LBSNs were discriminated. Many of them seemed to be functionally polarized and had separate input (=soma side) and output (= contralateral side) branches. Their role in the neural circuitry for the contralateral uropod motor pattern formation in response to the sensory stimulation of the tailfan was discussed.

INTRODUCTION

One of the most fruitful consequences of the intracellular recording and staining analyses in arthropod central nervous system has been the functional characterization of local non-spiking interneurons. Many of them function as pre-motor elements in the control of both rhythmic and episodic movement [1–4].

However, recent studies have demonstrated that not all the local interneurons are non-spiking. Spiking local interneurons are also found in various arthropod species [5–8 in cricket: 9–12 in locust: 13 in crayfish]. Their functions have so far been analyzed in terms of the sensory processing. For example, the "omega" cell is involved in cricket auditory system and seems to play a role in sound localization [e.g. 8]. On the other hand, some bilateral-type spiking local interneurons in crayfish have motor output as indicated by current injection experiment [13]. There is, however, only a small body of evidence which suggests their role as pre-motor elements.

We analyzed in this study the response of contralateral uropod motoneurons to the sensory stimulation of the tailfan. We show that at least four types of local bilateral spiking interneurons (LBSNs) contribute to transmit the sensory inputs across the midline and control the contralateral uropod motoneuron activity. The transmission of sensory inputs via these LBSNs has been investigated electrophysiologically.

Accepted May 23, 1985
Received May 16, 1985

MATERIALS AND METHODS

Animals and preparations

Adult male and female crayfish *Procambarus clarkii* Girard measuring 6 to 10 cm in length from

rostrum to telson were used in all experiments. The abdomen was isolated and pinned ventral side up in van Harreveld [14] solution. The dissection procedure has been described in detail previously [15]. The terminal (sixth) abdominal ganglion was exposed by removing the ventral aorta together with overlying connective tissue, and stabilized on a silver plate.

Extracellular recordings

Spike activity of the motoneurons innervating the uropod muscles was monitored by the extracellular oil-hook electrodes [16]. Activity of closer motoneurons was recorded from the second root motor bundle just proximal to its bifurcation to the reductor and to the adductor exopodite muscles. Activity of opener motoneurons was recorded from the third root motor bundle just distal to its bifurcation to the ventral rotator and the abductor exopodite muscles. In quiescent animals, both the closer reductor motoneuron No. 1 (Red MN No. 1) and one to four slow opener motoneurons were usually discharging spikes tonically.

Another extracellular oil-hook electrode was placed on the second root nerve bundle contralateral to the motoneuron recording side in order to stimulate the afferents which innervated the exopodite [17] electrically. In some preparations, oil-hook electrode for stimulation was also placed on the second root sensory bundle ipsilateral to the motoneuron recording side.

Intracellular recordings

Intracellular recordings were made in the terminal ganglion neuropil with microelectrodes filled with 3 or 5% solution of Lucifer yellow CH with 0.1 M lithium chloride [18] (resistance: >150 MΩ) or 2.5 M potassium acetate (resistance: 40–80 MΩ). The constant polarizing current could be injected into the penetrated cell through the recording electrode by a bridge circuit.

Following the physiological study, neuron morphology was obtained with Lucifer stain [19].

RESULTS

Contralateral uropod motor pattern formation

Either mechanical or electrical stimulation of the uropod on one side induced the reciprocal activation of the antagonistic motoneurons innervating contralateral uropod muscles. Spontaneous discharge frequency of the contralateral closer, Red MN No. 1 was increased and that of the opener motoneurons was decreased by light touches to the exopodite (Fig. 1A). This reciprocal motor activation was also elicited by electrical stimulation of the second root afferents (Fig. 1B–1). Even after the abdominal 5–6 connectives were cut, reciprocal motor pattern by the root shock remained essentially unaltered (Fig. 1B–2).

Structure and function of LBSNs

Neither the second root afferents nor the uropod

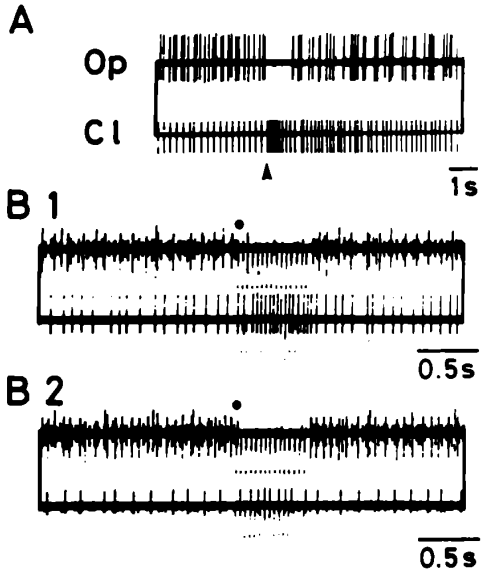

FIG. 1. Contralateral uropod motor pattern formation. A: Light touches to the exopodite (indicated with arrowhead) elicited the decrease in the discharge frequency of the opener motoneurons (1st trace) and the increase in that of the closer, Red MN No. 1 (2nd trace) on the contralateral side. B1: Electrical stimulation of the second root afferents (indicated with dot) elicited similar reciprocal motor activation. B2: Cutting the abdominal 5–6 connectives left the reciprocal motor pattern essentially unaltered. The shape of the Red MN No. 1's spike (2nd trace) changed due to the displacement of the electrode.

motoneuron dendrites did cross the midline of the terminal abdominal ganglion [15, 17, 20]. Thus, the sensory inputs from the exopodite must be transmitted via some intercalating neuron(s) to the contralateral uropod motoneurons.

One of possible candidates for intercalating neuron was local bilateral spiking interneuron (LBSN). Four types of structurally and physiologically distinct LBSNs were discriminated.

Type-I LBSN We twice penetrated type-I LBSN. This LBSN extended branches bilaterally (Fig. 2A). The branches on both sides were spatially separated and connected with an unbranched thin process. Main branches on the soma side were projected anteriorly, laterally and posteriorly within the ventral half, while those on the contralateral side extended only laterally and posteriorly within the dorsal half of the ganglion.

Type-I LBSN was usually silent in a quiescent animal. When the exopodite on the soma side was mechanically stimulated, the LBSN was activated through the second root afferents and the contralateral Red MN No. 1 also increased its spike activity (Fig. 2B). Electrical stimulation of the afferents also activated the LBSN: it responded with small (<8 mV) spike on large (>15 mV) EPSP (Fig. 2C). The latency from the stimulus to the EPSP onset was about 5.5 msec. Spikes of this LBSN elicited by 2 nA depolarizing current injection increased the contralateral Red MN No. 1 activity (Fig. 2D).

Type-II LBSN We penetrated five type-II LBSNs in different preparations. This LBSN displayed H-shape structure which is distinct from that of type-I LBSN. Fine branches on the soma side were smooth and those on the contralateral side had numerous varicosities (Fig. 3A).

This LBSN was also silent in a quiescent animal and received excitatory inputs from the second root afferents on the soma side. This responded with small (<4 mV) spike on large (>10 mV) EPSP (Fig. 3B–1). The latency was between 3.9 and 5.5 msec. This LBSN received inhibitory inputs from the second root afferents on the contra-

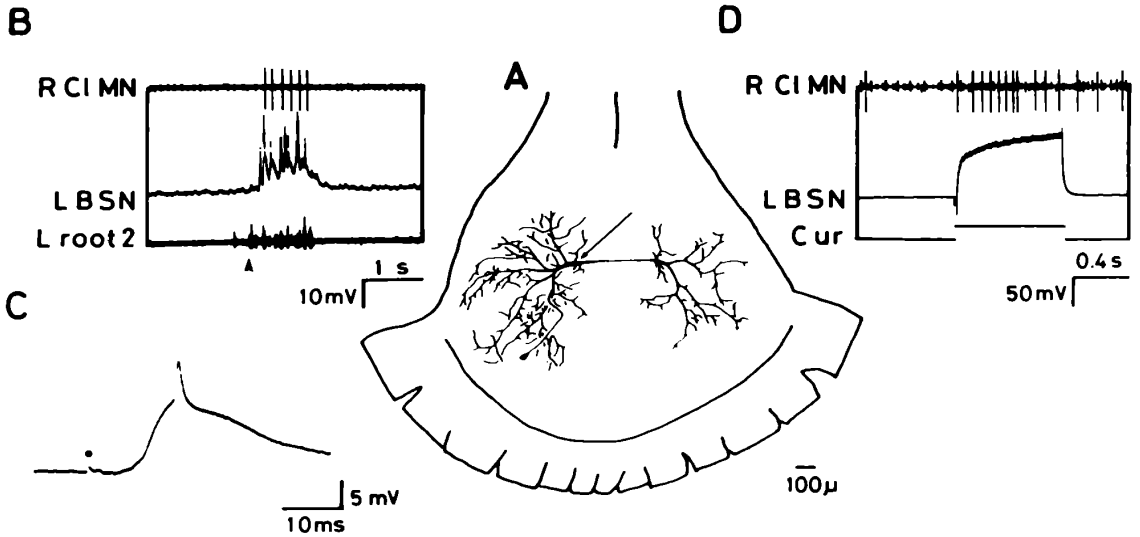

FIG. 2. Morphology and physiology of Type-I LBSN. A: Type-I LBSN stained with Lucifer yellow and viewd ventrally in a whole mount preparation. Anterior is to the top. Arrow: penetration site of the recording electrode (see [15]). B–C: Response of type-I LBSN to sensory stimulation. B: When the left exopodite was mechanically stimulated (arrowhead), the type-I LBSN (2nd trace) was activated through the left second root afferents (3rd trace) and the right Red MN No. 1 (1st trace) also increased its activity. C: Electrical stimulation (dot) of the left second root afferents also activated the LBSN. D: Effect of current injection into LBSN upon spike activity of Red MN No. 1. Intracellular injection of 2 nA depolarizing current (upward deflection in 3rd trace) into the LBSN (2nd trace) increased the spike frequency of the right Red MN No. 1 (1st trace).

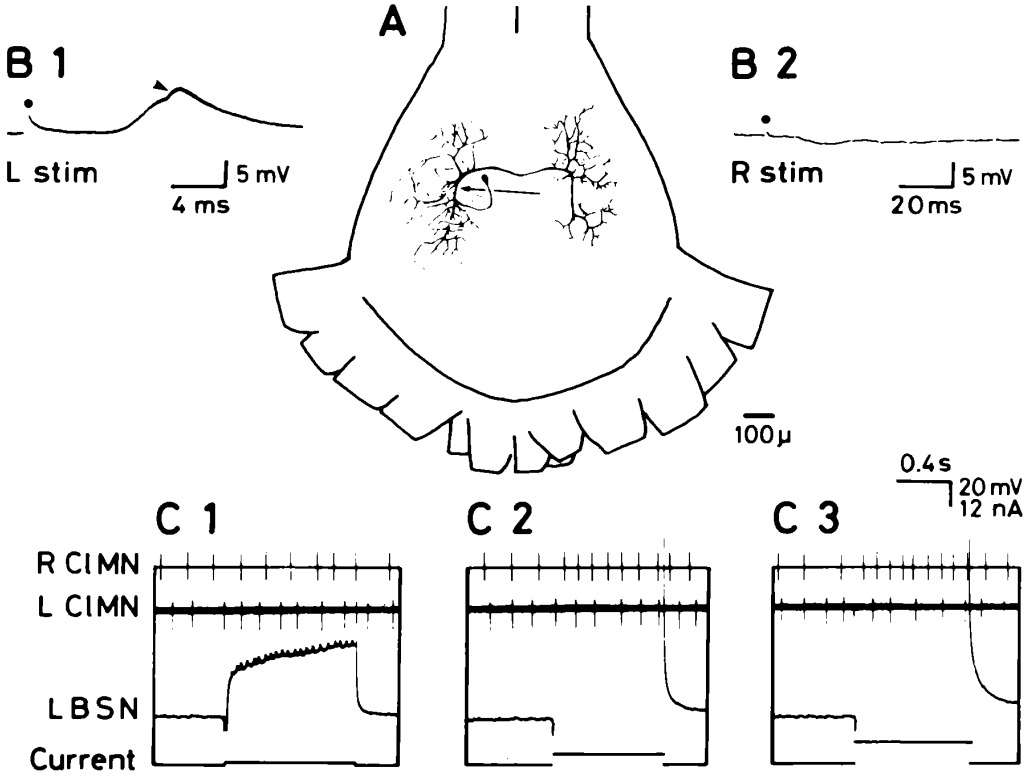

FIG. 3. Morphology and physiology of Type-II LBSN. A: Type-II LBSN viewed ventrally. Anterior is to the top. B: Response of type-II LBSN to sensory stimulation. B1: Electrical stimulation of the left second root afferents (dot) activated the LBSN. The LBSN responded with small spike (indicated with arrowhead) on large EPSP. B2: Electrical stimulation of the right second root afferents (dot) elicited the membrane hyperpolarization of the LBSN. C: Effect of current injection into LBSN upon spike activity of the Red MN No. 1 on both sides. C1: Intracellular injection of 1 nA depolarizing current (upward deflection in 4th trace) into the LBSN (3rd trace) slightly increased the spike frequency of the right Red MN No. 1 (1st trace). C2: With 5 nA depolarizing current, spike frequency of the right Red MN No. 1 was more increased. C3: Even with 10 nA depolarizing current, left Red MN No. 1 (2nd trace) showed no detectable change.

lateral side to the soma (Fig. 3B–2). The IPSP had rather small amplitude and long latency (=about 10 msec). Current injection revealed that this LBSN had postsynaptic effect only upon the Red MN No. 1 on the contralateral side to the soma. When 1 nA depolarizing current was injected, spike frequency of the Red MN No. 1 on the contralateral side was slightly increased (Fig. 3C–1). With 5 nA depolarizing current, it was more increased (Fig. 3C–2). However, we could not recognize any noticeable change in the spike activity of the ipsilateral Red MN No. 1 even with current of more than 10 nA (Fig. 3C–3).

Type-III LBSN Four type-III LBSNs were encountered. Their gross morphology was rather similar to that of type-I LBSN: main branches on the contralateral side to the soma were projected only laterally and posteriorly. However, physiologically, we classified them into two distinct classes. Type-III LBSN was spontaneously discharging spikes at the resting potential.

In two cases, we analyzed the response of the type-III LBSN to the bilateral sensory stimulation. In response to the root shock on the soma side, spontaneous spike discharge of both the LBSNs was increased (Fig. 4B–1). The EPSP could be easily distinguished by injecting 1 nA hyperpolarizing current (Fig. 4B–2). The latency was between 3.6 and 6.1 msec. But when the afferents on

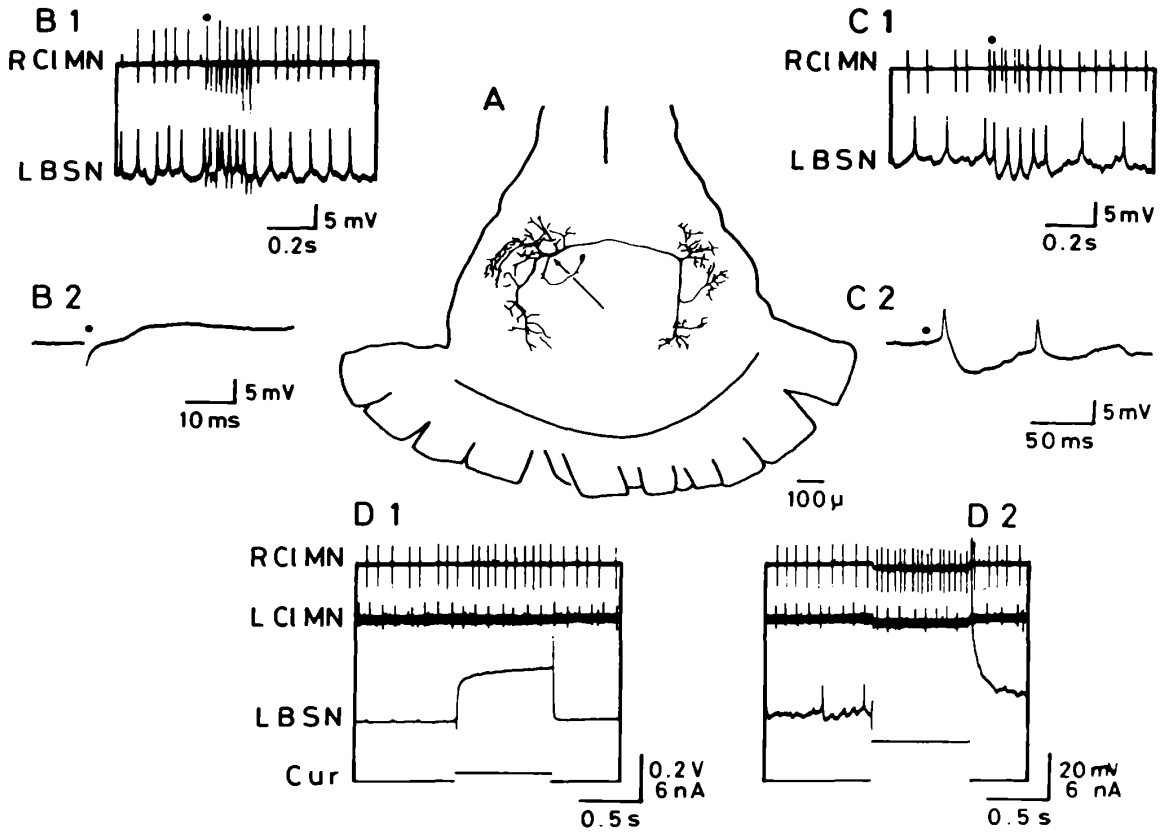

FIG. 4. Morphology and physiology of Type-III LBSN. A: Type-III LBSN viewed ventrally. Anterior is to the top. B–C: Response of type-III LBSN to sensory stimulation. B1: In response to the root shock (dot) on the left side, spontaneous spike discharge of the LBSN (2nd trace) was increased corresponding to the increase in the spike frequency of the right Red MN No. 1 (1st trace). B2: The EPSP was distinguished by the injection of 1 nA hyperpolarizing current into the LBSN. C1: In response to the root shock (dot) on the right side, the membrane potential of the LBSN was continuously hyperpolarized while the spikes followed each shocks. C2: The LBSN responded with spike first and then showed IPSP by the root shock (dot). D: Effect of current injection into LBSN upon spike activity of the Red MN No. 1 on both sides. D1: Injection of 1 nA depolarizing current (upward deflection in 4th trace) into the LBSN (3rd trace) increased the spike frequency of the right Red MN No. 1 (1st trace). D2: Even with 5 nA depolarizing current, left Red MN No. 1 (2nd trace) showed no detectable change.

the contralateral side were stimulated, only one of them showed hyperpolarizing response. Another one showed more complex membrane potential change. When the root shock was given, it responded with spike first and then showed slow (duration >100 msec) IPSP (Fig. 4C–2). The membrane potential was continuously hyperpolarized while the spikes followed each shocks (Fig. 4C–1). Injection of 1 nA depolarizing current into this LBSN increased the spike frequency of the Red MN No. 1 on the contralateral side only (Fig. 4D–1), the ipsilateral Red MN No. 1 showed no noticeable activity change even if 5 nA depolarizing current was injected (Fig. 4D–2).

Type-IV LBSN The LBSN of another structure was recorded just once. Soma was located at the ventral ridge of the postero-lateral portion of the ganglion (Fig. 5A). A fine process emerged from the soma and gave rise to the abundant arborization in the neuropil. Major branches were on the soma side, but some branches crossed the midline and projected into the contralateral half of the ganglion.

This LBSN was silent in a quiescent animal and was excited by the root shock on the soma side: this responded with 20 mV spike on 10 mV EPSP (Fig. 5B). The EPSP latency was about 7 msec. When 1 nA depolarizing current was injected,

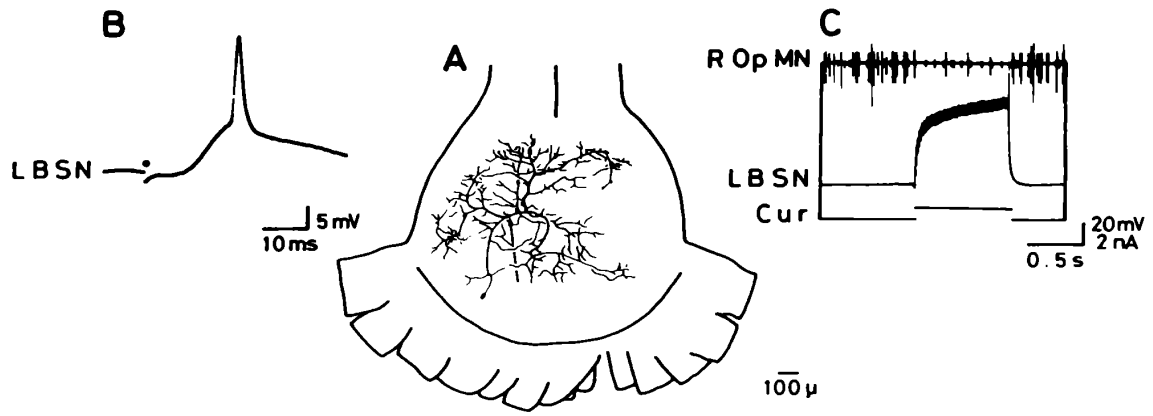

FIG. 5. Morphology and physiology of Type-IV LBSN. A: Type-IV LBSN viewed ventrally. Anterior is to the top. B: Electrical stimulation of the left second root afferents (dot) activated the LBSN. The LBSN responded with large spike on small EPSP. C: Intracellular injection of 1 nA depolarizing current (upward deflection in 3rd trace) into the LBSN (2nd trace) decreased the spike frequency of the right opener motoneurons (1st trace).

spike activity of the opener motoneurons on the contralateral side was decreased (Fig. 5C).

Synaptic events on uropod motoneurons

In response to the root shock, contralateral Red MN No. 1 showed a sustained change in membrane potential (Fig. 6A–1). This membrane depolarization (=5–10 mV) showed slow rising phase, long duration and gradual decline. The latency from the stimulus to the EPSP onset was variable in different preparations and in the range of 5.2–14.9 msec.

The synergistic, fast adductor motoneuron (Add MN) was also depolarized by the root shock. The latency was 4.9 to 8.6 msec (7.1±1.2 msec; n=8), and was on average about 1.5 msec longer than the mean latency of the EPSP occurring in the LBSNs (5.6±1.2 msec; n=11). In many cases, Add MN received compound EPSP which showed long duration. When the Add MN was depolarized intracellularly, EPSP amplitude was decreased. Conversely, EPSP amplitude was increased when hyperpolarizing current was injected (Fig. 6A–2).

Slow opener motoneuron, on the other hand,

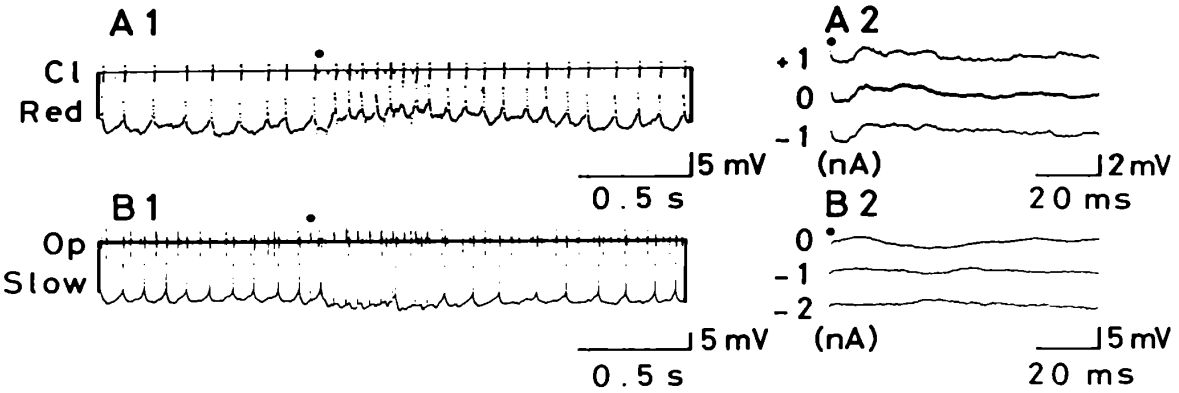

FIG. 6. Response of uropod motoneurons to sensory stimulation. A: Response of closer motoneurons. A1: In response to the root shock on the left side (dot), the right Red MN No. 1 showed sustained membrane depolarization. A2: Long, compound EPSP was recorded from the Add MN by the root shock (dot). EPSP amplitude was increased by hyperpolarization and decreased by depolarization at the site of recording. B: Response of opener motoneurons. B1: In response to the root shock on the left side (dot), the right slow opener motoneuron showed the sustained membrane hyperpolarization. B2: IPSP of the fast opener motoneuron by the root shock (dot) was reversed by the passage of hyperpolarizing current.

showed a sustained membrane hyperpolarization (=2–8 mV) in response to the root shock (Fig. 6B–1). The latency in different preparations was in the range of 8.3–19.8 msec. Fast opener motoneuron also received an IPSP. The IPSP amplitude was decreased by the injection of 1 nA hyperpolarizing current and reversed by 2 nA current (Fig. 6B–2). The latency was between 6.7 and 11.2 msec (8.5±1.3 msec; n=12) and was about 1.4 msec longer than the mean latency of the EPSP in the Add MN.

Synaptic events on LNSNs

Unilateral local non-spiking interneurons (LNSNs) also received sensory inputs from the contralateral second root afferents. Some LNSNs which made non-inverting connection to the Red MN No. 1 (Fig. 7A–1) received a depolarizing PSP and showed continuous membrane depolarization (=2–5 mV) in response to the root shock (Fig. 7A–2). This depolarization reflected an increase on the closer activity and a simultaneous decrease on the opener activity. Since the LNSNs' membrane potential change of only a few millivolts would be sufficient to produce a measureable change in transmitter release [21], these LNSNs could increase the Red MN No. 1 activity by receiving excitatory inputs from the contralateral afferents. The latency was between 4.6 and 8.2 msec (6.9±1.4 msec; n=5).

Other LNSNs which made inverting connection to the Red MN No. 1 (Fig. 7B–1) received a hyperpolarizing PSP showing continuous membrane hyperpolarization (=2–10 mV) when stimulated (Fig. 7B–3). The latency was variable and in the range of 9.5–33.4 msec. In many LNSNs (=75%) of inverting ones, artificial hyperpolarization increased the Red MN No. 1 activity (Fig. 7B–2).

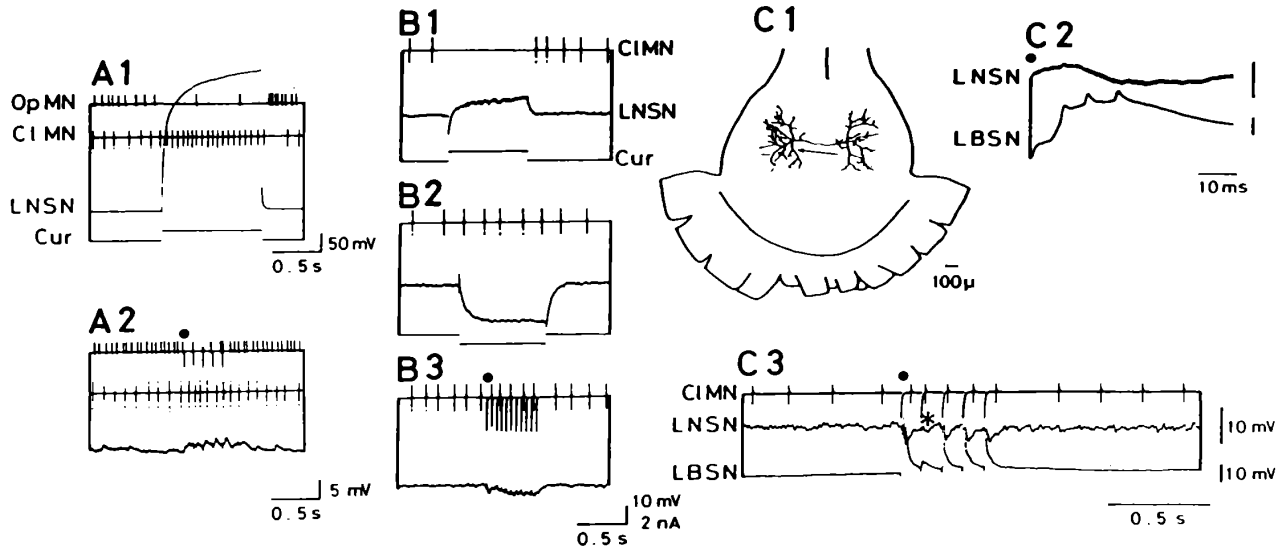

FIG. 7. Response of LNSNs to sensory stimulation. A: Response of a non-inverting LNSN. A1: Intracellular injection of 1 nA depolarizing current (upward deflection in 4th trace) into the LNSN on the right side (3rd trace) increased the spike frequency of the right Red MN No. 1 (2nd trace) and decreased that of the opener motoneurons (1st trace). A2: In response to the root shock on the left side (dot), the LNSN showed the continuous membrane depolarization corresponding to the increase in the Red MN No. 1 activity. B: Response of an inverting LNSN. B1: Injection of 1 nA depolarizing current into the right LNSN decreased the right Red MN No. 1 activity. B2: Injection of 1 nA hyperpolarizing current (downward deflection in 3rd trace) increased the Red MN No. 1 activity. B3: In response to the root shock on the left side (dot), the LNSN showed the continuous membrane hyperpolarization corresponding to the increase in the Red MN No. 1 activity. C: Simultaneous intracellular recordings from the LBSN and the inverting LNSN. C1: Morphology of recorded type-II LBSN. C2: Electrical stimulation of the left second root afferents (dot) elicited the membrane hyperpolarization of the LNSN (upper) and the membrane depolarization of the LBSN (lower). C3: Correlation between the spike activity of the LBSN and the membrane potential change of the LNSN. The PSP amplitude of the LNSN (2nd trace) was very small when the type-II LBSN (3rd trace) failed to produce a spike following the root shock (dot) which increased the Red MN No. 1 activity (1st trace).

Thus, their continuous membrane hyperpolarization by the root shock was also responsible to the increase in the Red MN No. 1 activity.

After physiological characterization of the inverting LNSN, type-II LBSN (Fig. 7C–1) was impaled by the second electrode and simultaneously recorded. Since the latency from the stimulus to the onset of the LBSN PSP was about 4 msec and that of the LNSN was about 11 msec (Fig. 7C–2), there seems to be no direct connection between them. However, a close correlation was found between the LBSN's spike activity and the LNSN's membrane potential change (Fig. 7C–3). The PSP amplitude of the LNSN was very small when the type-II LBSN failed to produce a spike following the root shock (asterisk in Fig. 7C–3).

DISCUSSION

The reciprocal activation of the contralateral uropod motoneurons in response to the sensory stimulation of the second root afferents was formed by the local circuitry within the terminal abdominal ganglion since it could be reproduced even after abdominal 5–6 connectives were cut (Fig. 1B). Irrespective of animals' size or sex, this reciprocal motor pattern was almost exclusively elicited. In only 11 cases of 263 preparations (4%), we observed exceptional reversal activation: opener motoneurons were excited and Red MN No. 1 was inhibited.

Functional characterization of LBSNs

Four types of structurally and physiologically distinct local bilateral spiking interneurons (LBSNs) were discriminated in this study (Table 1). They extended branches bilaterally in the ganglion. They received excitatory inputs from the second root afferents on the soma side. Their artificially elicited spike activity increased the discharge frequency of closer Red MN No. 1 and decreased that of opener motoneurons on the

TABLE 1. Summary of the functional and structural characteristics of the LBSNs

type	I	II	III	IV
numbers encountered	2	5	4	1
input				
soma side	EPSP	EPSP	EPSP	EPSP
opposite side	?	IPSP	IPSP*	?
spike rate				
(spike/EPSP>1)	NO	NO	NO	YES
spont discharge	NO	NO	YES	NO
output				
soma side	NO	NO	NO	?
contra side	YES	YES	YES	YES
bridge	YES	YES	YES	NO
branching pattern				
soma side				
anterior	YES	YES	YES	YES
lateral	YES	YES	YES	YES
posterior	YES	YES	YES	NO
opposite side				
anterior	NO	YES	NO	YES
lateral	YES	YES	YES	NO
posterior	YES	YES	YES	YES

? Not examined.
*only 1 case received both excitatory and inhibitory inputs (see Fig. 4).

contralateral side. We hence concluded that these LBSNs serve in transmission of the sensory inputs across the midline and formation of the reciprocal activity pattern of the contralateral uropod motoneurons.

Type I–III LBSNs showed a common basic structure that their branches on both sides were spatially separated. In many cases, they only received excitatory inputs from the afferents on the soma side and affected the uropod motoneurons on the contralateral side. They usually responded with less than 5 mV spike on EPSP of more than 15 mV, while type-IV LBSN which did not display separate bilateral branches responded with more than 20 mV spike on less than 10 mV EPSP (cf. Figs. 2 and 5). Although not all the LBSNs were analyzed in regard of the bilateral input-output relation and we did not record the LBSNs on the contralateral side to their somata, the obtained morphological and physiological results supported the idea that these LBSNs are functionally polarized and had separate input (=soma side) and output (=contralateral side) branches as preliminarily suggested by Reichert *et al.* [13].

However, the structural types of the LBSNs shown in this paper are not exhaustive. Reichert *et al.* [13] have reported several other structures of the LBSNs in the same ganglion. It is, therefore, possible to assume that there are other functional types of the LBSNs in the ganglion.

Input connection to LBSNs

The latency from the stimulus to the onset of the EPSP was between 3.6 and 7.4 msec (5.6±1.2 msec; n=11). In 5 preparations, we intracellularly recorded the second root afferent. The average conduction velocity of the afferents was 1.2± 0.3 m/sec. Since the distance between the point of stimulating the second root nerve bundle and the point at which second root enters the ganglion was 3 to 6 mm, 2.5 to 5 msec delay can be estimated. If we assume the conduction time of the afferent spike within the ganglion, the value of the LBSNs' latency would be reasonable to postulate the monosynaptic connection between the afferents and the LBSNs. Furthermore, EPSP latency of the one of identifiable local non-spiking interneurons, LDS [19, 20] was 4.2 to 7.4 msec (5.4± 1.1 msec; n=6) in this study. Since the LDS was assumed to receive the synaptic inputs monosynaptically from the uropod [22], the similar value of the mean latency of the LBSN (Table 2) also supported the monosynaptic nature of the afferent-LBSN synapse. Further detailed study such as simultaneous recordings from the afferent and the LBSN is yet needed to clarify this point.

Output connection from LBSNs

The mean latency of both the EPSP in the Add MN and the depolarizing PSP in the non-inverting LNSN was very similar and on average about 1.5 msec longer than the mean latency of the EPSP occurring in the LBSNs (Table 2). If we assume that this was the conduction time necessary for the sensory inputs from the LBSNs to cross the midline and arrive at its synaptic site to the postsynaptic neurons on the contralateral side, the synaptic delay should be less than 1 msec. Both the Add MN and the non-inverting LNSNs thus seem to receive the sensory inputs monosynaptically from the LBSN.

In the Red MN No. 1, however, it was frequently difficult to distinguish a discrete PSP from its slow membrane depolarization and its EPSP laten-

TABLE 2. Comparison of latency from the second root afferents to the various inter- and motoneurons

type	number	mean latency (ms)
LBSN	11	5.6±1.2<3.6–7.4>[d]
LDS	6	5.4±1.1<4.2–7.4>
Closer MN		
Add MN	8	7.1±1.2<4.9–8.6>
Red MN	5 (4)[c]	10.9±3.8<5.2–14.9>
Opener MN		
fast MN	12	8.5±1.3<6.7–11.2>
slow MN	9 (4)	12.4±3.5<8.3–19.8>
LNSN		
d-PSP[a]	5 (3)	6.9±1.4<4.6–8.2>
h-PSP[b]	8 (3)	14.9±7.6<9.5–33.4>

[a] Depolarizing PSP-evoke LNSN.
[b] Hyperpolarizing PSP-evoke LNSN.
[c] Very weak response following single electric root shock.
[d] Minimum and maximum value.

cy was variable among preparations (Table 2). This must be attributed to both the parallel pathway connection in the circuitry and the electrode penetration site. Since some Red MN No. 1 showed the similar value of the latency to that of the Add MN, the Red MN No. 1 also seems to receive the sensory inputs monosynaptically from the LBSN. However, since the dendritic branches of the Red MN No. 1 was rather thinner than those of the Add MN [15], delayed potential change via LNSNs might be only observed by the fortuitous electrode penetration. Compared the latency between both the opener motoneurons and the inverting LNSNs and the LBSNs (Table 2), the connection between them seems to be not monosynaptic but at least one neuron is intercalated.

Thus, the LBSN made polysynaptic connections with the closer motoneurons via some kinds of the LNSNs in parallel with the monosynaptic connection. Since the injection of current pulse into LNSNs could produce the smooth and long-lasting membrane potential change of the postsynaptic motoneurons in a graded manner [23, 24], delayed pathways via LNSNs contributed to form the sustained changes in membrane potential of the uropod motoneurons.

The parallel pathway connection via the LNSNs have now been found in some motor systems in arthropod central nervous system [11, Takahata and Hisada in preparation]. Intercalation of the LNSNs in the circuitry would be advantageous to generate the adequate patterns of the motoneuron activity since the LNSNs could exert the analog control over the membrane potential of the postsynaptic neurons [e.g. 24]. Unfortunately, we could not demonstrate in full, in this paper, direct causality between the LBSN and the LNSN (Fig. 7) since the probability of obtaining successful simultaneous intracellular recording of the LBSN and the LNSN was prohibitingly low. However, to determine the interaction between them and to clarify the functional role of LBSNs of each types, further detailed analyses by the simultaneous recordings from them would be indispensable.

ACKNOWLEDGMENTS

We thank our colleagues, especially Dr. M. Takahata for many helpful criticisms and suggestions during the course of this work. This work was supported by Grants-in-Aid from the Ministry of Education, Science and Culture to M.H. (Nos. 58124027, 59340046, 59540447).

REFERENCES

1 Pearson, K. G. and Fourtner, C. R. (1975) Nonspiking interneurons in walking system of the cockroach. J. Neurophysiol., **88**: 33–52.

2 Burrows, M. and Siegler, M. V. S. (1976) Transmission without spikes between locust interneurones and motoneurones. Nature, **262**: 222–224.

3 Heitler, W. J. and Pearson, K. G. (1980) Nonspiking interactions and local interneurones in the central pattern generator of the crayfish swimmeret system. Brain Res., **187**: 206–211.

4 Takahata, M., Nagayama, T. and Hisada, M. (1981) Physiological and morphological characterization of anaxonic non-spiking interneurons in the crayfish motor control system. Brain Res., **226**: 309–314.

5 Casady, G. B. and Hoy, R. R. (1977) Auditory interneurons in the cricket *Teleogryllus oceanicus*: physiological and anatomical properties. J. Comp. Physiol., **121**: 1–13.

6 Popov, A. V., Markovich, A. M. and Andjan, A. S. (1978) Auditory interneurons in the prothracic ganglion of the cricket, *Gryllus bimaculatus* deGeer. I. The large segmental auditory neuron (LSAN). J. Comp. Physiol., **126**: 183–192.

7 Wohlers, D. W. and Huber, F. (1978) Intracellular recording and staining of cricket auditory interneurons (*Gryllus campestris* L., *Gryllus bimaculatus* DeGeer). J. Comp. Physiol., **127**: 11–28.

8 Wohlers, D. W. and Huber, F. (1982) Processing of sound signals by six types of neurons in the prothoracic ganglion of the cricket, *Gryllus campestris* L. J. Comp. Physiol., **146**: 161–173.

9 Burrows, M. and Siegler, M. V. S. (1982) Spiking local interneurons mediate local reflexes. Science, **217**: 650–652.

10 Burrows, M. and Siegler, M. V. S. (1984) The morphological diversity and receptive fields of spiking local interneurons in the locust metathoracic ganglion. J. Comp. Neurol., **224**: 483–508.

11 Siegler, M. V. S. and Burrows, M. (1983) Spiking local interneurons as primary integrators of mechanosensory information in the locust. J. Neurophysiol., **50**: 1281–1295.

12 Siegler, M. V. S. and Burrows, M. (1984) The morphology of two groups of spiking local interneurons in the metathoracic ganglion of the locust. J. Comp. Neurol., **224**: 463–482.

13 Reichert, H., Plummer, M. R., Hagiwara, G., Roth, R. L. and Wine, J. J. (1982) Local inter-

neurons in the terminal abdominal ganglion of the crayfish. J. Comp. Physiol., **149**: 145–162.

14 Van Harreveld, A. (1936) A physiological solution for freshwater crustaceans. Proc. Soc. Exp. Biol. Med., **34**: 428–432.

15 Nagayama, T., Takahata, M. and Hisada, M. (1983) Local spikeless interaction of motoneuron dendrites in the crayfish *Procambarus clarkii* Girard. J. Comp. Physiol., **152**: 335–345.

16 Wilkens, L. A. and Wolfe, G. E. (1974) A new electrode design for en passant recording, stimulation and intracellular dye injection. Comp. Biochem. Physiol., **48**: 217–220.

17 Calabrese, R. L. (1976) Crayfish mechanoreceptive interneurons: I. The nature of ipsilateral excitatory inputs. J. Comp. Physiol., **105**: 83–102.

18 Stewart, W. W. (1978) Functional connections between cells as revealed by dye-coupling with a highly fluorescent naphthalimide tracer. Cell, **14**: 741–759.

19 Hisada, M., Takahata, M. and Nagayama, T. (1984) Structure and output connection of local non-spiking interneurons in crayfish. Zool. Sci., **1**: 41–49.

20 Reichert, H., Plummer, M. R. and Wine, J. J. (1983) Lateral inhibition mediated by a non-spiking interneuron: Circuit properties and consequences for behavior. J. Physiol., Paris, **78**: 786–792.

21 Burrows, M. (1979) Synaptic potentials effect the release of transmitter from locust nonspiking interneurons. Science, **204**: 81–83.

22 Reichert, H., Plummer, M. R. and Wine, J. J. (1983) Identified nonspiking local interneurons mediate nonrecurrent, lateral inhibition of crayfish mechanosensory interneurons. J. Comp. Physiol., **151**: 261–276.

23 Burrows, M. and Siegler, M. V. S. (1978) Graded synaptic transmission between local interneurones and motor neurones in the metathoracic ganglion of the locust. J. Physiol., London, **285**: 231–255.

24 Nagayama, T., Takahata, M. and Hisada, M. (1984) Functional characteristics of local non-spiking interneurons as the pre-motor elements in crayfish. J. Comp. Physiol., **154**: 499–510.